COBEM-2019-2241
CORROSION BEHAVIOR OF A SPRAY FORMED CU-AL-NI-MN SHAPE MEMORY ALLOY

Edelize Angélica Gomes
Vanessa de Freitas Cunha Lins
Mechanical Engeneering Department, Federal University of Minas Gerais, Antonio Carlos Avenue 6627, Zip Code 31270901.
edelizeg@hotmail.com, vlins@deq.ufmg.br

Eric Marchezini Mazzer
Metallurgical and Materialsl Engeneering Department, Federal University of Minas Gerais, Antonio Carlos Avenue 6627, Zip Code 31270901.
eric.marchezini@demet.ufmg.br

Abstract. Shape Memory Alloys (SMA) have some exceptional properties, such as shape memory effect and superelasticity. Both are associated with a martensitic/austenitic phase transformation. Alloys of the Cu-Al-Ni, Cu-Zn-Al and NiTi systems belong to this class of material. Interest in the study of Cu as the SMA base arises from the fact that they are cheaper than NiTi and can achieve better properties in specific applications. In this way, the electrochemical properties of the Cu-Al-Ni-Mn system processed by spray conformation in 3.5% m/v NaCl solution were measured by electrochemical impedance spectroscopy. The samples surface was examined by optical microscope, SEM, XRD and EDS methods. The results showed the impedance modulus increased with the immersion time due to the continuous growth of the passive film on the alloy surface. The XRD and EDS analysis showed the presence of copper, aluminium, nickel and magnesium compounds, Cu-oxides, Cu-chlorides and Mn-oxides on alloy surface. This system attracts the attention of the scientific community because it is a good candidate for the application of high temperature shape memory alloys (HTSMA), operating above 100 ° C.

Keywords: corrosion, Cu-Al-Ni-Mn shape memory alloy, electrochemical impedance spectroscopy

1. INTRODUCTION

The research related to intelligent materials and structures has received increasing attention due to its high scientific and technological significance. Shape Memory Alloys (SMA) are an important branch of smart materials. The term "shape memory alloy" refers to the group of metallic materials that have ability to return to some shape or size defined when subjected to thermal cycling. Among the many alloying systems that have SMA, Ni-Ti alloys, Cu-Al-Ni and Cu-Zn-Al have been studied and are commercially exploited. SMA have a remarkable capacity for application in several technical areas, from robotics to aerospace, which makes them a multifunctional material, since they are very useful as actuators and sensors as shown in literature (MohdJane et al., 2014). Among shape memory alloys, Ni-Ti alloys have been used in variety of applications, including biomedical and industrial applications. However, the low processing temperatures (-100 to 100°C) and high production costs of Ni-Ti alloys make their use for many applications impractical, especially for use in high temperatures. Thus, Cu-Al-Ni alloys become a better option in relation to Ni-Ti alloys, since they have high transformation temperatures, low production costs and a higher thermal stability (Zárubová et al., 2008).

Among the alloys with copper-based SMA, the main ones are the Cu-Zn and Cu-Al alloys. The presence of a third or fourth element allows the adjustment of the transformation temperatures, which are very dependent on the chemical composition, besides being able to improve the mechanical and functional properties of the alloy stability. Studies have shown that the Cu-Al alloy is unsuitable for most practical applications because of high martensitic transformation temperatures (between 300 and 500 ° C), but these temperatures can be reduced to 180 °C by the addition of up to 4 wt.% of nickel. On the other hand, Cu-Al-Ni alloys are considerably cheaper than Ni-Ti alloys being a suitable option when high martensitic transformation temperatures and stability are required. Recently, literature reports the study of the corrosion behavior of the Cu-Al-Ni SMA with the addition of 0.25% by mass of Ag, by means of electrochemical tests in 3.5% w/v NaCl solution. Cu-Al-Ni alloys have a lower corrosion potential and a higher corrosion current density compared to Cu-Al-Ni-Ag alloys. The higher corrosion resistance of the alloys with Ag was attributed to the formation of corrosion products such as CuCl, silver chloride (AgCl), cuprous oxide (Cu_2O), aluminum oxide /

hydroxide (Al_2O_3 / Al $(OH)_3$) and silver oxide (Ag_2O) on the surface of the electrode, which acts as a barrier against aggressive agents (Safaa *et al*., 2014).

Zare and Ketabchi, (2016) evaluated the effect of Cr addition on the microstructure, transformation temperatures, mechanical and corrosion properties of Cu-Al-Ni alloy. They subjected the alloys with and without chromium to a thermomechanical treatment which included hot rolling, annealing and hydraulic pressing passages. In addition, tensile tests, differential scanning calorimetry and potentiodynamic polarization were performed to compare the properties of the alloys. For this, they used four samples of the alloy with different concentrations of Cr. The results showed that the chromium element acts as a grain refiner in this alloy, restricting grain growth. The potentiodynamic polarization test was performed to evaluate the corrosion behavior of Cu-Al-Ni in NaCl solution 3.5% m/v. Despite the adequate effect of Cr on corrosion behavior, increased deformation applied increased the corrosion rate. Both the addition of Cr and the higher value of the degree of deformation reduced the transformation temperature of austenite to martensite.

The alloys of the Cu-Al-Ni system with SMA induce special interest because of the advantageous alternative over the Ni-Ti or Cu-Zn and Cu-Zn-Al alloys due to economic issues, and ease of manufacturing. In addition, Cu-Al-Ni alloys do not lose the shape memory effect at temperatures above 100 °C such as Ni-Ti alloys (Wez *et* al., 2010)

This work contributes to the deepening of information related to the evaluation of the mechanical and electrochemical properties of an alloy processed by spray forming, which is an innovative technique, since such processing has inherent advantages compared to other routes such as:

• Obtaining a refined microstructure, usually with equiaxed grains of the order of 10-100 μm, with low segregation, precipitated second phases, eutectic and refined intermetallic phases. The alloys processed by spray forming may have metastable phases and a solubility in the solid phase. Therefore, subsequent thermal treatments allow a better control of precipitation in the matrix for optimization of mechanical properties.

• Possible production of near net shape products, with formats close to the shape of the final product, such as tubes, rollers, tapes, being more advantageous than conventional casting or powder metallurgy by accommodating in a single process several required steps.

• Processing of alloys difficult to obtain by other methods such as alloys based on Al, Pb, Cu, Mg, Ni, Ti, Co and some steels.

The purpose of this work is to investigate the corrosion behavior of Cu-Al-Ni-Mn with different immersion times in a 3.5 wt.% NaCl solution and its microstructural analysis to contributes to the deepening of information related to the evaluation of the electrochemical properties of an alloy processed by spray forming.

2. METHODOLOGY

2.1 Alloy Processing

The shape memory alloy with nominal composition memory Cu-11.35Al-3.2Ni-3.5Mn (% by mass) was produced at the Federal University of São Carlos, using elements of high purity (> 99.9%) through the casting in a crucible coated with silica-alumina refractory in an induction furnace with an argon lance on the molten metal. Then, still in the liquid state, the metal was processed by the spray-forming technique. In this process, the metal is poured into a tundish, which directs the flow of metal into a chamber where atomization occurs through the passage of an inert gas. This interacts with the metal forming drops. The formation of the ingot occurs by the interruption of these drops by a substrate, forming a deposit. Subsequently, this deposit was cut and machined into the desired formats. The atomizing gas used was nitrogen (N_2) with a pressure of 0.5 MPa and a 6 mm atomization nozzle. The initial material load was 4 kg. Subsequently, specimens with 10 mm diameter and 0.5 mm thickness were cut and machined. The samples were used to evaluate the effect of this process on the corrosion behavior of the alloy in a saline medium.

2.2 Immersion and Eletrochemical Tests

The immersion tests were performed in a saline aqueous solution of 3.5% w/v NaCl. Three samples were made for each immersion period. The samples were immersed in a saline solution after 1, 24, 48, 72, 148, 190, 238, and 286 hours.

The samples with a surface area of 0.54 cm^2 were used for electrochemical tests. The test was conducted at 25°C. Before each analysis, the sample was mechanically polished with 800, 1200, 4000 mesh, cleaned in isopropyl alcohol, rinsed with water and immersed in the test solution. A glass cell containing 3.5% w/v NaCl solution was mounted using the AUTOLAB 100 potentiostat. A three-electrode cell was used for the electrochemical tests, where the reference electrode was the saturated calomel electrode (SCE), the platinum was the counter electrode and the sample was the working electrode. Open circuit potential measurements were performed for one hour or until potential stabilization.

Electrochemical impedance investigations were carried out with amplitude of ± 10 mV around the corrosion potential and frequency range from 100 kHz to 5 mHz. The tests were performed in triplicate.

2.3 Materials characterization

The micrographs of Cu-Al-Ni-Mn shape memory alloy before electrochemical testing were obtained by optical microscopy. The samples were previously mechanically polished with different grit emery papers, degreased in isopropyl alcohol and immersed for a few seconds in a solution of ferric chloride in order to reveal the microstructural details.

XRD (X-ray diffraction) patterns were recorded by an X-ray diffractometer, PHILIPS, model PW 1710, equipped with Cu tube, CuKα radiation and graphite monochromator crystal, after corrosion testing in 286 h immersion period. The surface energy dispersive spectra (EDS) of alloy was characterized by scanning electron microscope (SEM, JSM6360, JEOL, Tokyo, Japan) instrument, after corrosion testing in 286 h immersion period.

3. RESULTS AND DISCUSSION

3.1 Impedance measurements

The experimental impedance spectra obtained, at OCP, with the material Cu–Al–Ni-Mn shape memory alloy, exposed to 3.5 wt.% NaCl at different intervals of immersion are shown as Nyquist and Bode plots in Fig. 1 and Fig.2 respectively.

The response of the system in the Nyquist complex plane Fig.1 consists of two time constants. The impedance (Z) increased as the immersion time increased, which indicates a decrease in the corrosion rate of Cu-Al-Ni-Mn with time.

The Bode diagram is shown in Fig.2. At high frequencies (f> 1 kHz), the impedance is the electrolyte resistance. In the region of average frequency, the linear log | Z | vs. log f relates to the slope near -1 and the phase angle of ≈-60∘ determine the capacitive behavior of the system for higher immersion times. In the lower frequencies, the phase angle of ≈-25∘ and slope of the log | Z | vs log f near -0.5 pointed to the presence of diffusion process. It can be seen that the overall impedance of the system increases with the immersion time, which indicates that the surface of the electrode gets more protection. The development of more than one time constant is deduced by the inspection of the spectra, which reflect the diversity of the phenomenon, which occurs in the system under investigation (Alfantaz *et* al., 2009 Badawy *et* al., 2009).
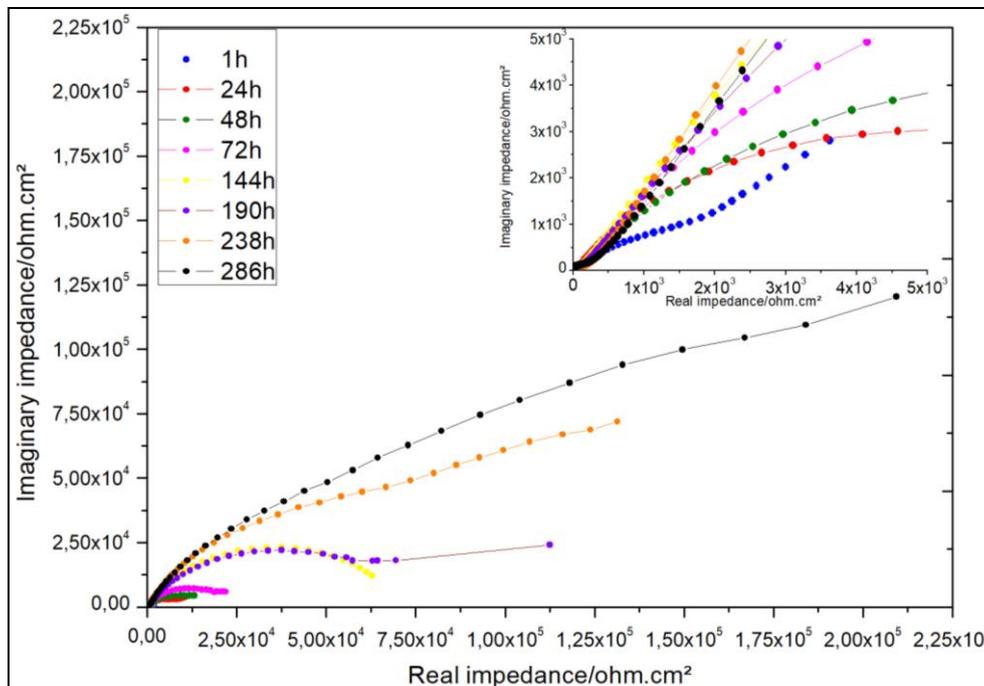

Figure 1. Niquyst plots of Cu-Al-Ni-Mn alloy after different times of immersion in 3.5% w/v NaCl solution.
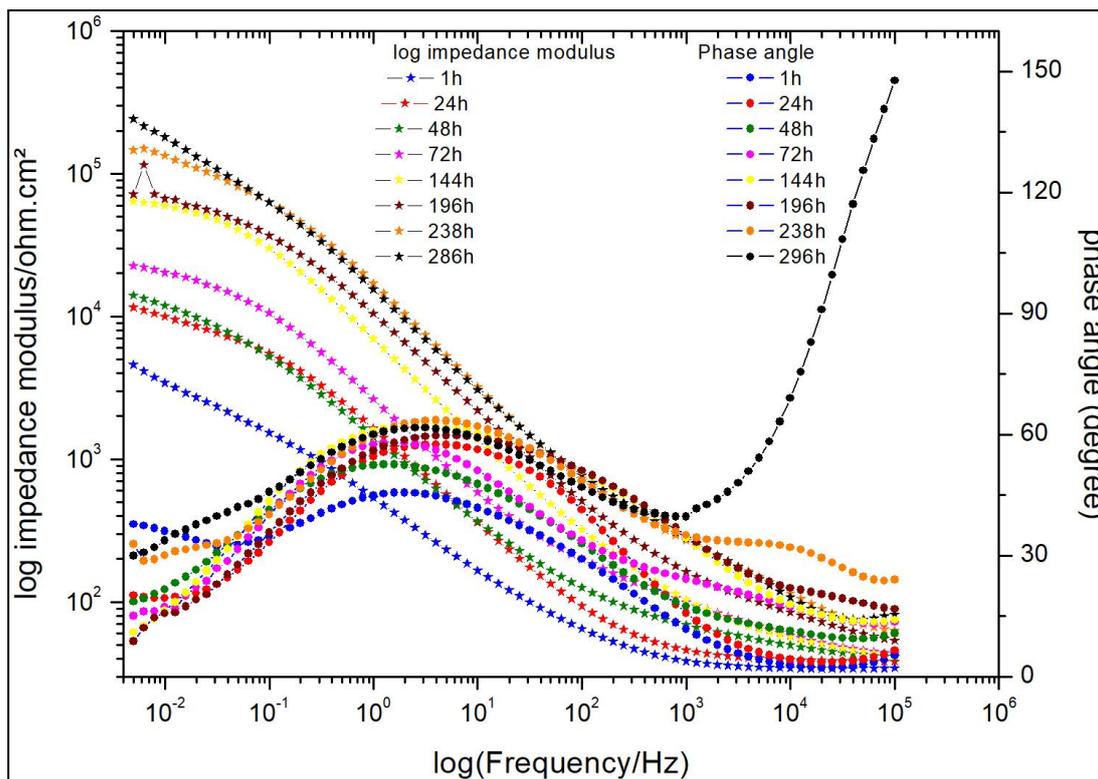
Figure 2. Bode plots of Cu-Al-Ni-Mn alloy after different times of immersion in 3.5% w/v NaCl solution.

From the respective phase angle Bode plots in Fig. 2, two phase maxima were present, the major one at intermediate frequencies (between 1 and 10) and the other at low frequencies, such behavior indicates the presence of two time constants representing the processes. The phase maxima were attributed to the protective oxide film and the phase maximum at low frequency range corresponds to the electrical double layer. The changes in the phase maximum with time indicate the differences in the relaxation time constants at different exposure times. From the corresponding phase angle Bode plots, it can be seen that the angle values at the intermediate frequency zone increase with the immersion time, which indicates a decrease in the corrosion rate of the alloy with time. The total impedance magnitude values of the Cu-Al-Ni-Mn increases with the increase in exposure time implying an increase in the corrosion resistance due to the growth of the passive film till the steady state is achieved. This could be attributed to the Ni segregation, where Ni^{2+} from the alloy dissolution incorporated into the crystal lattice of Cu_2O and the number of cation vacancies decreases with increasing the nickel content (Blundy *et* al., 1972, Beccaria and Crousier,1989), which represents not inconsiderable ratio about 10% from the alloy content. Segregation into the Cu_2O barrier layer occurs via a solid state reaction and Ni^{2+} interacts with mobile cation vacancies which leads to a decrease in the ionic conductivity and an increase in the electronic conductivity of the barrier film leading to a higher corrosion resistance (Urquidi *et* al., 1985, Metikos *et* al.,2011).

3.2 Microstructure and surface analysis

The surface of the electrodes before electrochemical experiments was examined with optical microscope, SEM and EDS analysis and the results are presented in Figs. 3 and 4. As can be seen from optical and scanning electron micrographs of the Cu–Al–Ni-Mn alloy in Figs. 3 and 4, the microstructure includes grains with martensite plates. The parallel bands in martensite can be considered twin-like martensite, which is confirmed by SEM micrographs shown in Fig. 4(b). The chemical composition of the investigated alloy was obtained using EDS analysis in Fig. 4(a). Also, after corrosion testing, surface morphologies of the three selected specimens were investigated with SEM, EDS and XRD.
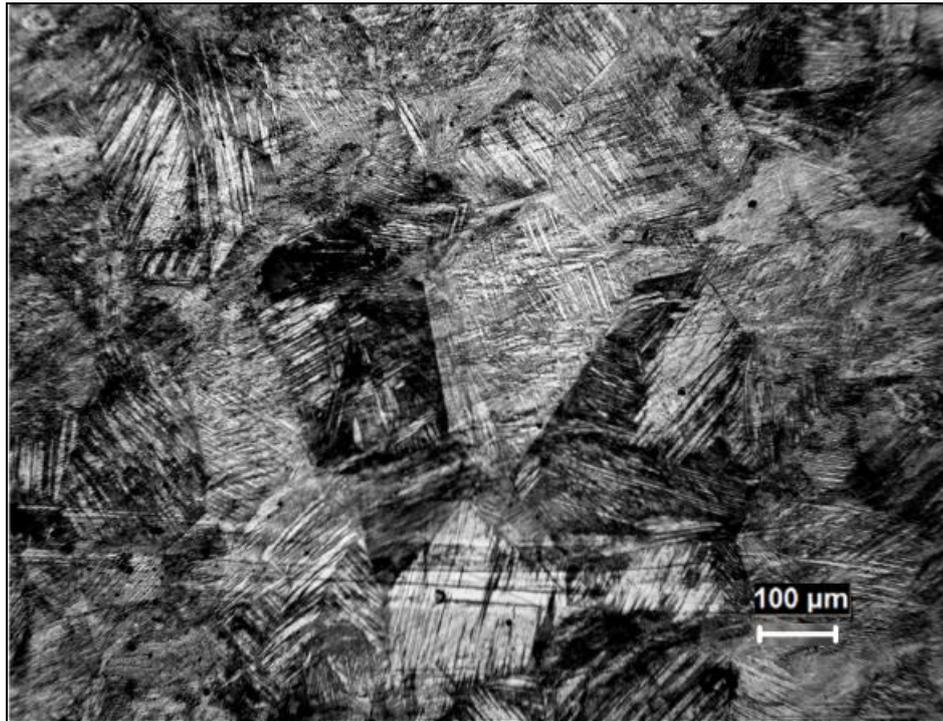
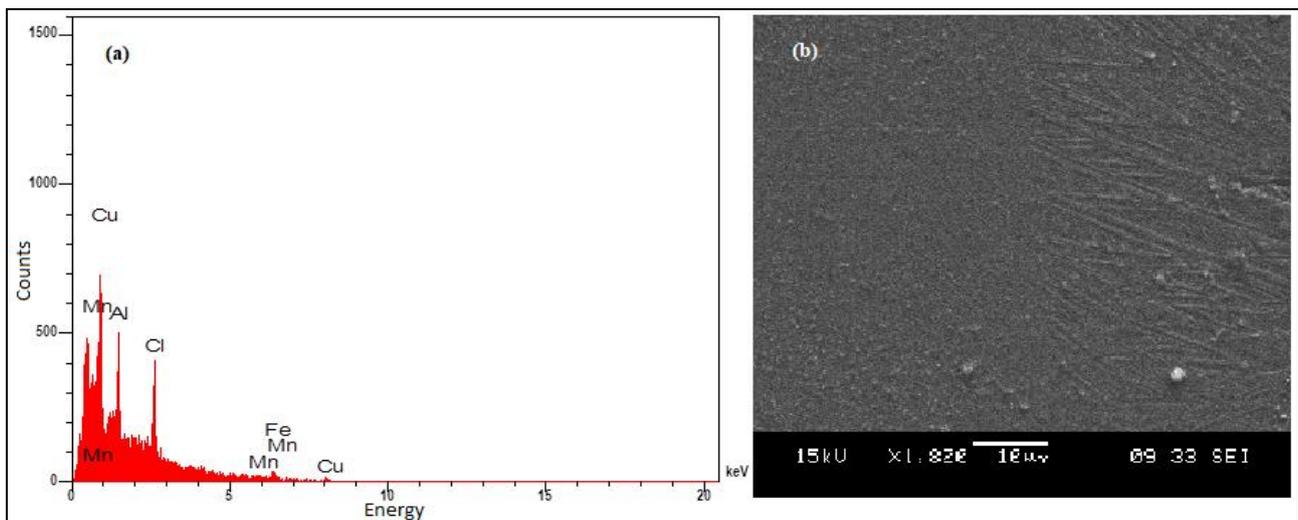Figure 3. Optical micrograph of Cu–Al–Ni-Mn shape memory alloy before electrochemical testing.

Figure 4. EDS results (a) and SEM micrograph (b) and of Cu–Al–Ni-Mn alloy before electrochemical testing.

As can be seen from micrographs, the microstructure includes grains and martensite plates in Fig. 3. The grains clearly appear and martensite plates have different orientations within particular grains. As it is well known, martensite is formed primarily as the needle-like shape and martensite is the typical morphology for Cu–Al–Ni shape memory alloys (Gojic et al., 2011).

The SEM and EDS analyses were used to characterize the morphology of Cu–Al–Ni-Mn alloy after an electrochemical study. Also, the EDS analysis was used to show the chemical elements of corrosion products (surface attack) which were formed on the surface of the specimen after corrosion testing. Typical SEM micrographies for the alloy are shown in Fig. 5(b) and the EDS analyses of Cu–Al–Ni-Mn alloy after impedance measurement of alloy immersed by 286 h in 3.5wt.% NaCl solution are shown in Fig. 5(a).

The presence of oxygen on the alloy surface can be explained by the formation of Cu_2O and $Al(OH)_3$ layers on the electrode surface (Otmaci et al., 2004, Milic et al., 2008). By investigating the corrosion behaviour of pure Cu and Cu-alloys in solutions containing Cl^- ions, it was established that at least two different corrosion products can be found at the electrode surface, i.e. CuCl and Cu_2O (Deslouis et al., 1988, Otmaci et al., 2004, Milic et al., 2008). The CuCl

surface layer formed rapidly on the electrode surface, while the Cu_2O layer formed after a longer immersion period by hydrolysis of CuCl (Deslouis *et* al., 1988, Otmaci *et* al., 2004, Milic *et* al., 2008).
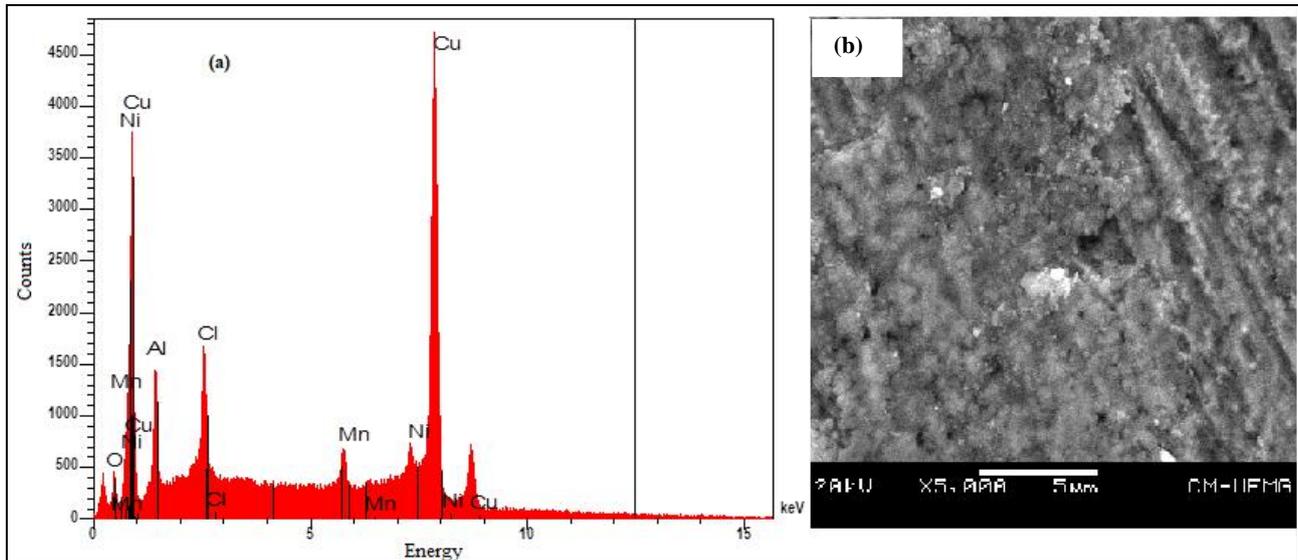

Figure 5. SEM micrograph (b) and EDX(a) results and of Cu-Al-Ni-Mn alloy after electrochemical testing.

Figure 6 shows the XRD patterns of the Cu-Al-Ni-Mn specimens after 286 hours of immersion in 3.5 wt.% NaCl solution. The XRD analysis further confirmed the existence of CuCl, CuO, Mn_2O_3, $CuMnO_2$, $Mn(ClO_4)$ on the surface of the sample beside Cu reflections. The strong diffraction intensities of $CuMnO_2$ and Mn_2O_3 phases in Cu-Al-Ni-Mn SMA also indicate the formation of a Mn-oxide layer on the specimen surface in Fig. 5(a).
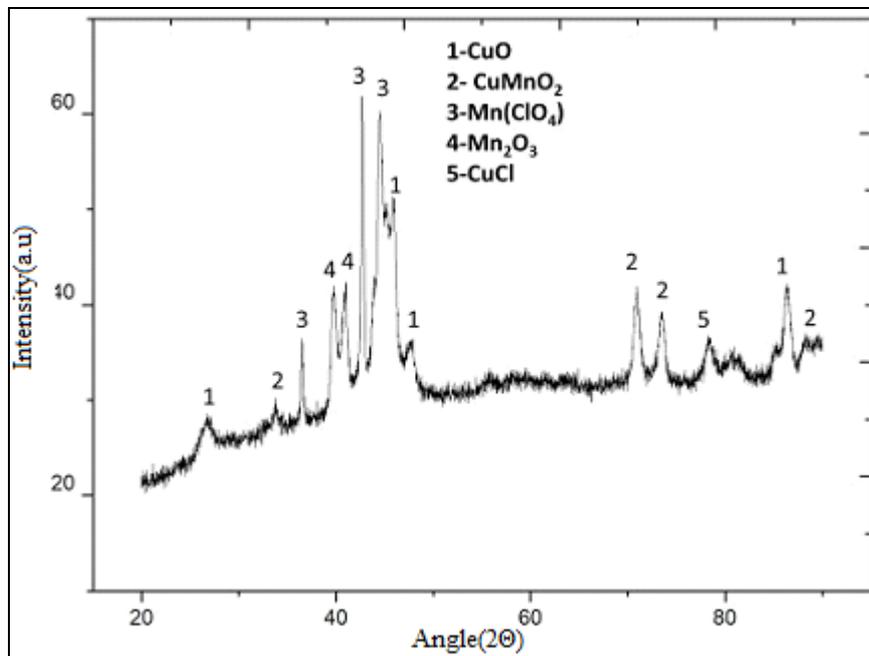

Figure 6. XRD patterns of Cu-Al-Ni-Mn alloy after immersion exposure in 3.5% NaCl for 286 h.

4. CONCLUSION

The corrosion behavior of the Cu-Al-Ni-Mn shape memory alloy was studied. The impedance had a small increase until 72 hours, and thus increased one magnitude order until 190 hours. From one hour of immersion until 286 hours of immersion, the impedance of shape memory alloy increased two magnitude orders.

Optical and scanning electron microscopy analysis prior to electrochemical testing showed the presence of grains with martensite plates in microstructure.

Microstructures after corrosion testing demonstrated the occurrence of corrosion products on the Cu–Al–Ni-Mn alloy surface. The EDS analyses revealed the presence of copper, aluminum, magnesium and nickel oxides and chlorides on the alloy surface. It was confirmed by XRD analysis, which indicates the presence of CuCl, CuO, Mn_2O_3, $CuMnO_2$ and $Mn(ClO_4)$ compounds.

5. ACKNOWLEDGEMENTS

6. REFERENCES

Alfantazi, A.M., Ahmed, T.M., Tromans, D., 2009. "Corrosion behavior of copper alloys in chloride media," *Material and Design.* Vol.30, pp. 2425–2430.

Badawy, El-Sherif, W.A., Shehata, R.M. H., 2009. "Electrochemical stability of Cu–10Al–5Ni alloy in chloride–sulfate electrolytes," *Electrochimca Acta*. Vol.54, pp. 4501–4505.

Beccaria, A.M., Crousier, J., 1989. "Dealloying of Cu-Ni alloys in natural sea water", *British Corrosion Journal.*Vol.24, pp. 49-52.

Deslouis C., Tribollet, B., Mengoli, G., Musiani, M.M., 1988. "Electrochemical behaviour of copper in neutral aerated chloride solution. II. Impedance investigation". *Journal off Applied. Electrochemistry.* Vol. 18, pp. 384–393.

Gojic, M., Vrsalovic, L., Kozuh , S., Kneissl , Al., Anzel , I., Gudic , S., Kosec, B., Kliski , M., 2011. "Electrochemical and microstructural study of Cu–Al–Ni shape memory alloy". *Journal of Alloys and Compounds*. Vol. 509, pp. 9782–9790.

Metikos, M., Hukovi´c, R., Babi´c, I., Skugor, Z., Grubac Z., 2011. "Copper–nickel alloys modified with thin surface films: Corrosion behaviour in the presence of chloride ions". *Corrosion Science*. Vol. 53, pp. 347-352.

Milic, S.M., Antonijevic, M.M., Serbula, S.M., Bogdanovic, G.D., 2008. "Influence of benzotriazole on corrosion behaviour of CuAlNiSi alloy in alkaline medium,". *Corrosion Engeneering Science Technology*. Vol. 43, pp. 30–37.

MohdJani, J., Leary, M., Subic, A., Gibson, M.A., 2014. "A review of shape memory alloy research, applications ad opportunities," *Materials& Design*. Vol. 56, pp. 1078-1113.

Otmaci, H., Telegdi, J., Papp, K., Stupnisek-Lisac, E., 2004. "Protective properties of an inhibitor layer formed on copper in neutral chloride solution". *Journal off Applied. Electrochemistry.* Vol. 34, pp. 545–550.

Safaa N. Saud, E. Hamzah, T. Abubakar, H.R. Bakhsheshi-Rad, Farahany, S,. Abdolahi, A., Taher, M.M., 2014. "Influence of Silver nanoparticles addition on the phase transformation, mechanical properties and corrosion behaviour of Cu–Al–Ni shape memory alloys," *Journal of Alloys and Compounds*. Vol. 612, pp. 471–478.

Urquidi, M., Macdonald, D.D., 1985. "Solute-Vacancy Interaction Model and the Effect of Minor Alloying Elements on the Initiation of Pitting Corrosion" *Journal of the Electrochemical Society*. Vol. 132, pp. 555-558.

Wez, Z.G., Sandstromand, R., Miyazaki, S, 1998. "Review Shape Memory Materials and Hybrid Composites for Smart Systems," *Journal of Materials Science.* Vol. 33, Nº. 15, pp. 3743- 3762.

Zare, M., Ketabchi M., 2016. "Effect of chromium element on transformation, mechanical and corrosion behavior of thermomechanically induced Cu–Al–Ni shape memory alloys," *Journal of Thermal Analysis & Calorimetry*. Vol. 127, pp. 2113-2123.

7. RESPONSIBILITY NOTICE

The authors are the only responsible for the printed material included in this paper.